Science Advances
AAAS

Supplementary Materials for

BRN2 as a key gene drives the early primate telencephalon development

Xiaoqing Zhu, Yicheng Guo, Chu Chu, Dahai Liu, Kui Duan, Yu Yin, Chenyang Si, Yu Kang, Junjun Yao, Xuewei Du, Junliang Li, Shumei Zhao, Zongyong Ai, Qingyuan Zhu, Weizhi Ji*, Yuyu Niu*, Tianqing Li*

*Corresponding author. Email: litq@lpbr.cn (T.L.); niuyy@lpbr.cn (Y.N.); wji@lpbr.cn (W.J.)

Published 4 March 2022, *Sci. Adv.* **8**, eabl7263 (2022)
DOI: 10.1126/sciadv.abl7263

The PDF file includes:

Other Supplementary Material for this manuscript includes the following:

Supplemental Figures

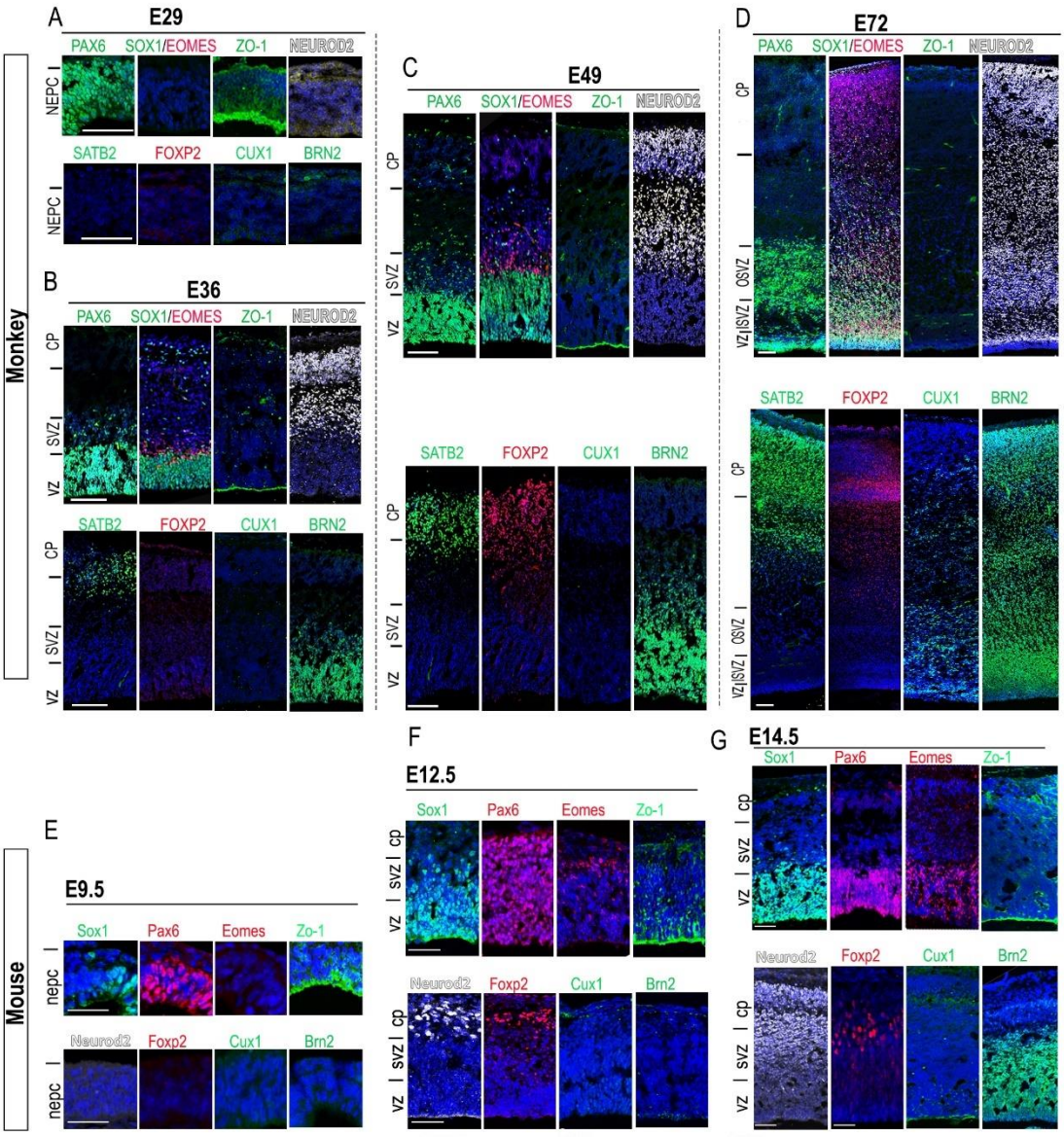

Fig. S1. The cell development stages and gene expression patterns over monkey cortical development. (A-D) Expression patterns of neural progenitor markers (PAX6, SOX1, EOMES and ZO-1) and the differentiated neuron markers (NEUROD2, SATB2, FOXP2, CUX1 and BRN2) in monkey primary somatosensory cortex across four different cortical development stages (E29 (**A**), E36 (**B**), E49(**C**), E72(**D**)). (**E-G**） Microphotographs of the coronal transects of mouse visual cortex immunostained with PAX6, SOX1, EOMES, ZO-1,

NEUROD2, FOXP2, CUX1 and BRN2 from E9.5 to E14.5: E9.5(**E)**, E12.5 (**F)** and E14.5 (**G)**. Scale bars: A, E, 50μm; others, 100μm. NEPC, neuroepithelium cells; VZ, ventricular zone; SVZ, subventricular zone; CP, cortical plate; OSVZ, outer SVZ; ISVZ, inner SVZ. Blue: DAPI, nuclear staining.

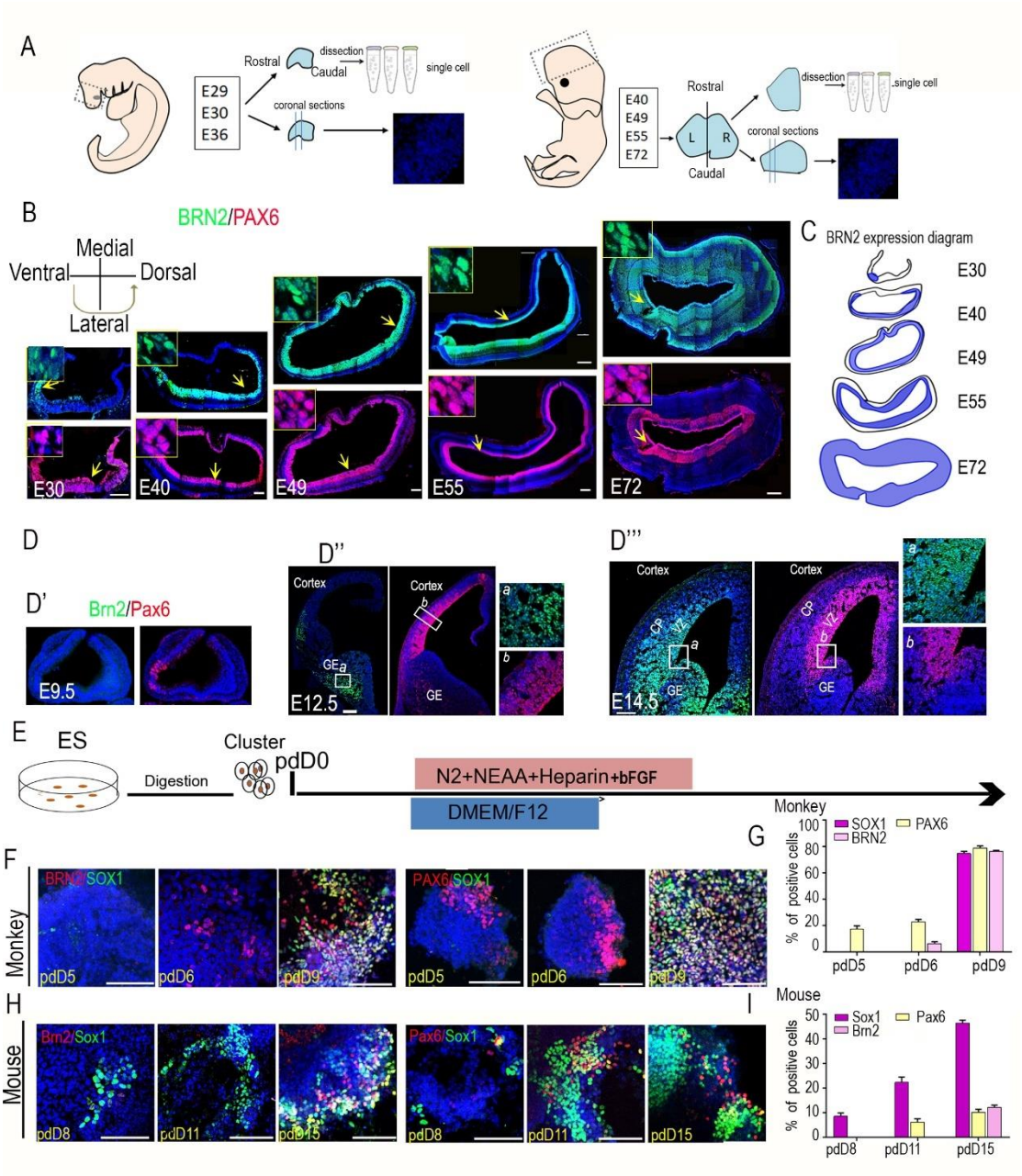

Fig. S2. Spatiotemporal distribution differences of BRN2 in mouse and monkey cortex, relative to Figure 1. (**A**) Schematic illustrating shows methods of section and dissection of the

monkey brain. (**B**) Dynamic expressions of BRN2 and PAX6 over monkey fetal cortical development, showing that BRN2 was initially expressed in lateral NEPCs at embryonic day 30 (E30), gradually extended along the VZ and spread across the entire cortex at E72. NEPCs, neuroepithelial cells; ISVZ, inner SVZ; OSVZ, outer SVZ; CP, cortical plate. (**C**) Diagram of dynamic BRN2 expression (green) over monkey fetal cortical development. (**D**) Brn2 and Pax6 expression in the E9.5 (D'), E12.5 (D'') and E14.5 (D''') mouse cortex, respectively. (**E**) Schedule of neural differentiation from ESCs induced by the bFGF condition. (**F**) Representative images of SOX1, PAX6 and BRN2 expressions in differentiated cells from monkey ESCs in the presence of bFGF. (**G**) Quantification of SOX1+, PAX6+ and BRN2+ cells during neural induction of monkey ESCs in the presence of bFGF. Data were presented as mean ± SEM (n=5). (**H**) Representative images of SOX1, PAX6 and BRN2 expressions in differentiated cells from mouse ESCs in the presence of bFGF. (**I**) Dynamics of $SOX1^+$, $PAX6^+$ and $BRN2^+$ cells during the neural induction of mouse ESCs in the presence of bFGF. Data were represented as mean ± SEM (n=5). pdD2: Day 2 post-differentiation. Scale bars: 100 μm. Blue: DAPI, nuclear staining.

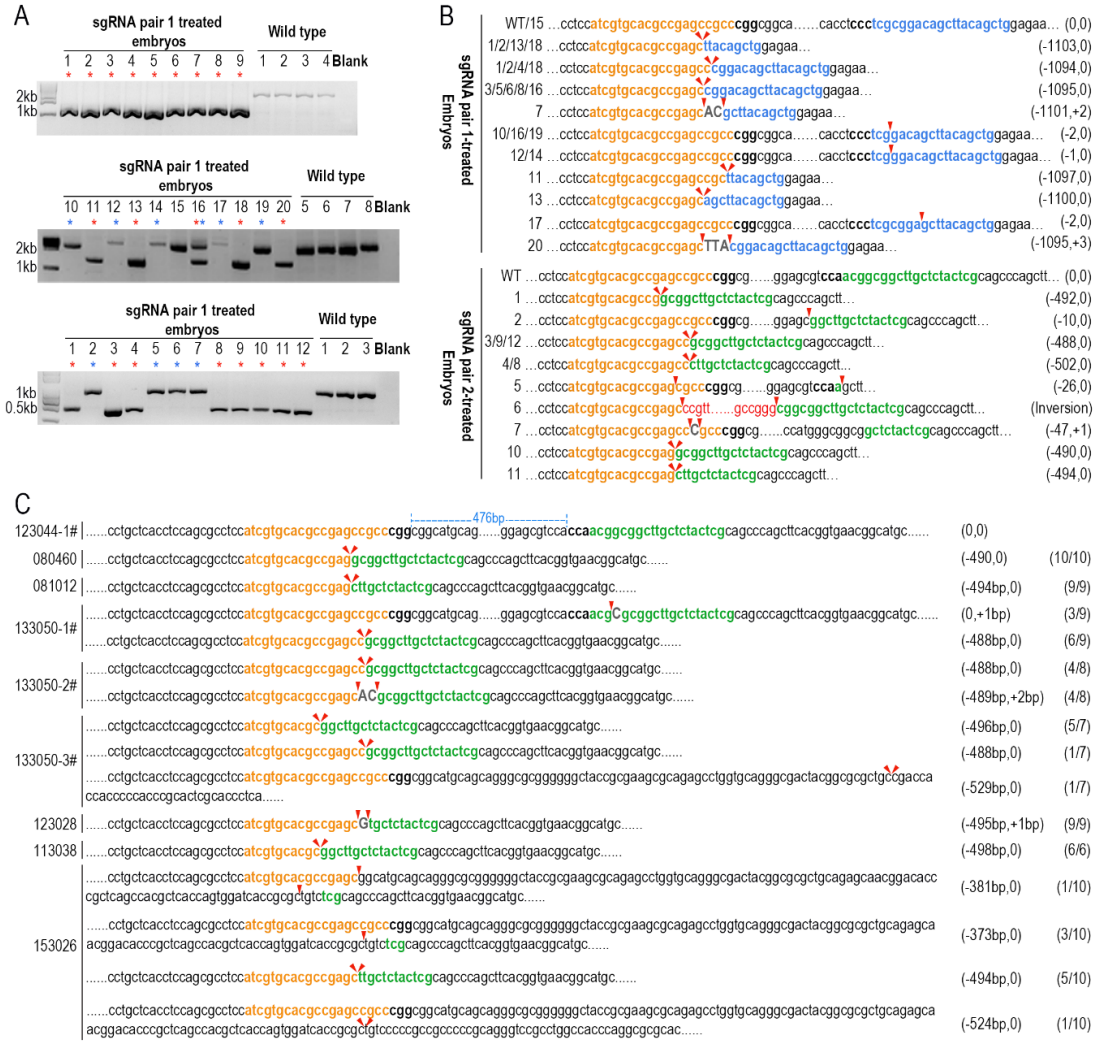

Fig. S3. **Genotype identifications of gene-editing embryos and fetuses using a CRISPR-Cas9 system, relative to Fig. 2**. (**A**) AGE (agarose gel electrophoresis) of the PCR products from BRN2 gene-editing and wild-type embryos. Red and blue asterisks indicate mutant embryos with indels and large deletion, respectively. Wild-type (*BRN2*+/+), embryos without RNP treated; (**B, C**) Sanger sequencing results of all examined embryos (**B**) and mutant fetuses (**C**). The wild-type fetus (123044) was used as the control. The red arrows indicate the location of Cas9-induced double-strand breaks. Bold black bases show the PAM (protospacer adjacent motif) sites. Dotted lines represent the omitted sequence. Red words show the inverted sequence after gene editing. The targeting sequences of sgRNA-A, sgRNA-B and sgRNA-C were labeled as orange, blue and green, respectively.

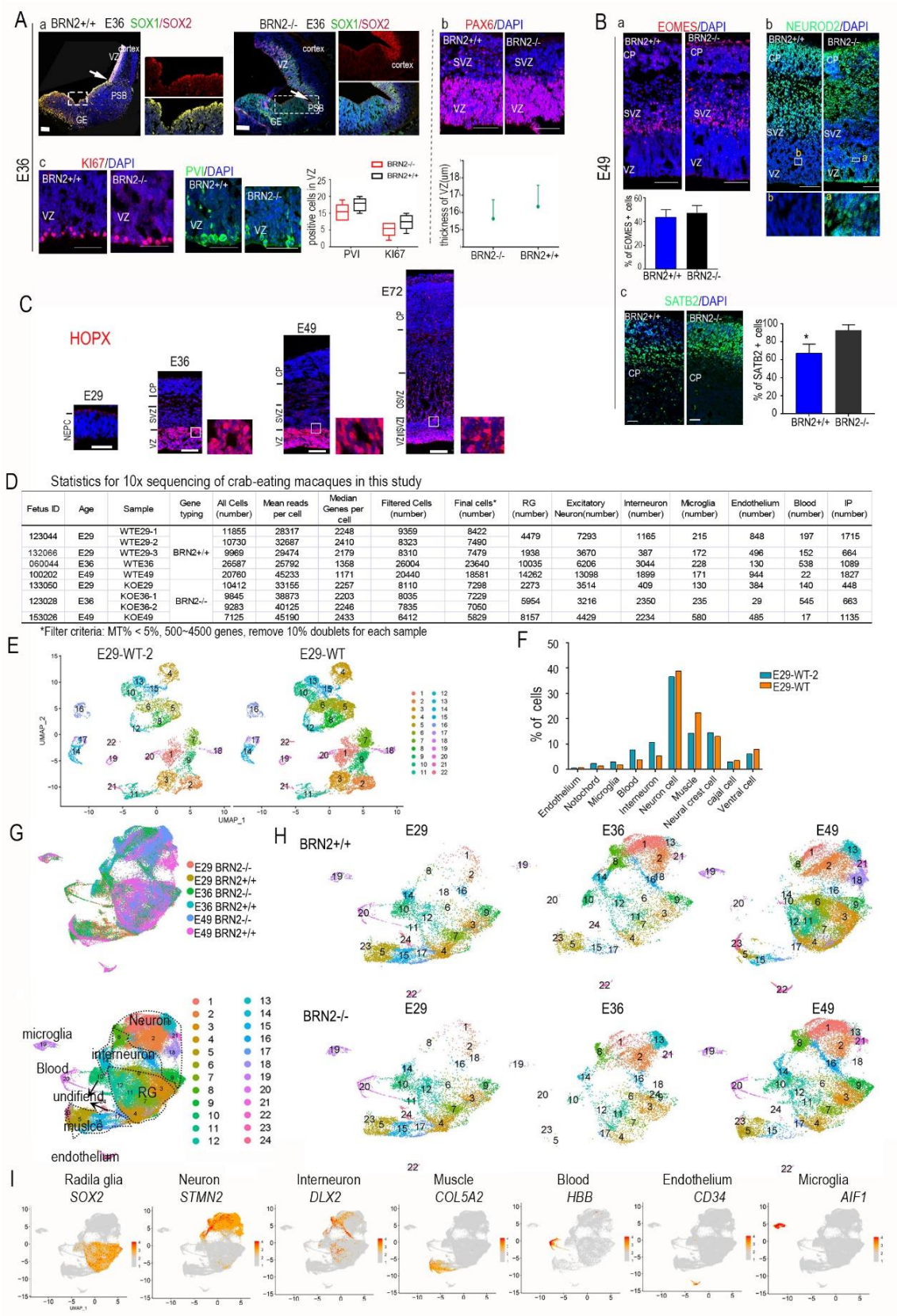

Fetus ID	Age	Sample	Gene typing	All Cells (number)	Mean reads per cell	Median Genes per cell	Filtered Cells (number)	Final cells* (number)	RG (number)	Excitatory Neuron(number)	Interneuron (number)	Microglia (number)	Endothelium (number)	Blood (number)	IP (number)
123044	E29	WTE29-1		11855	28317	2248	9359	8422							
		WTE29-2		10730	32687	2410	8323	7490	4479	7293	1165	215	848	197	1715
132066	E29	WTE29-3	BRN2+/+	9969	29474	2179	8310	7479	1938	3670	387	172	496	152	664
060044	E36	WTE36		26587	25792	1358	26004	23640	10035	6206	3044	228	130	538	1089
100202	E49	WTE49		20760	45233	1171	20440	18581	14262	13098	1899	171	944	22	1827
133050	E29	KOE29		10412	33155	2257	8110	7298	2273	3514	409	130	384	140	448
123028	E36	KOE36-1	BRN2-/-	9845	38873	2203	8035	7229							
		KOE36-2		9283	40125	2246	7835	7050	5954	3216	2350	235	29	545	663
153026	E49	KOE49		7125	45190	2433	6412	5829	8157	4429	2234	580	485	17	1135

Fig. S4. The transcriptome of single cells from BRN2-KO (*BRN2*-/-) and WT (*BRN2*+/+) telencephalon. (**A**) Immunostaining of SOX1, SOX2 (a), PAX6 (b), PVI and KI67 (c), in the

BRN2+/+ and *BRN2*-/- developing telencephalon at E36. Quantification of the thickness of VZ in *BRN2*-/- and *BRN2*+/+ cortex (b). Data were presented as mean± SEM, n = 4 representative images. Quantification of the number of KI67+ cells in VZ (mean ± SEM; n = 6 slices, >100 cells counted for each group). P>0.05, no significant difference was found. Scale bars: 100μm. (**B**) Immunostainings of intermediate progenitor markers EOMES, and cortical neuron markers (NEUROD2 and SATB2) in the *BRN2*+/+ and *BRN2*-/- developing telencephalon at E49. The ratios of EOMES+ and SATB2+ cells were quantified. Data were presented as mean ± SEM; n=8 representative images, >500 cells counted per group. * p<0.05, no significance in BRN2-/- and *BRN2*+/+ cortex. (**C**) Immunostaining of HOPX in the developing cortical germinal zone across different development stages. Scale bars: 100μm. (**D**) The table summarizing the information of single cells for all samples in the study. RG, radial glia; IP, intermediate progenitor. WT, wild-type (*BRN2*+/+) monkey fetus; KO, Knockout (*BRN2*-/-) monkey fetus. E29, embryonic day 29. (**E**) UMAP analysis of single cells from the two E29 donors, respectively. (**F**) Quantification of the cell proportions of 22 clusters reveal no significant difference in cell type compositions between the two E29 donors. (**G**) UMAP plots of single cells from the three *BRN2*+/+ and three *BRN2*-/- samples, respectively. (**H**) The UMAP plots from each stage. (**I**) Identification of cell types using canonical markers on the UMAP plots generated from (**G**).

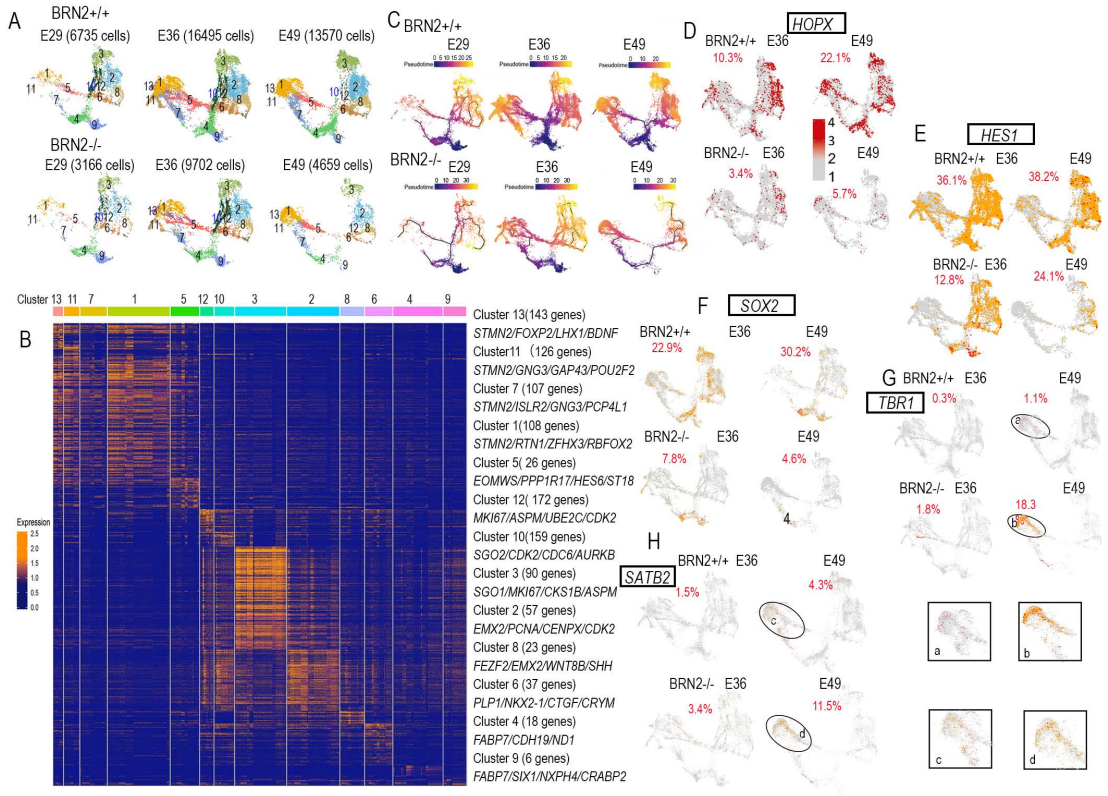

Fig. S5. ***BRN2* deficiency results in decreased expansion and precocious differentiation of radial glial cells (RGCs) in ventricular zone** (**A**) Subclustering of all integrated RGC, IP and ExN single cells from *BRN2*+/+ and *BRN2*-/- samples across three different developmental stages, respectively. (**B**) Differentially expressed genes among 13 clusters from *BRN2*+/+ and *BRN2*-/- samples. Please see Table S3. Representative genes from each cluster were shown on the right panel. (**C**) UMAP visualization of the cell trajectories, colored by inferred pseudo time, of *BRN2*+/+ and *BRN2*-/- samples across three different stages. (**D-H**) UMAP plots of *HOPX* (**D**), *HES1* (**E**), *SOX2* (**F**), *TBR1* (**G**), *SATB2* (**H**), expressions in the *BRN2*+/+ and *BRN2*-/- cortical cells across three different stages, respectively. (a-d) The magnification pictures of TBR1 positive cells in G and STAB2 positive cells in H. Numbers in red indicate the ratios of positive cells versus the total cell numbers, normalized expression value > 1. Blue: DAPI, nuclear staining.

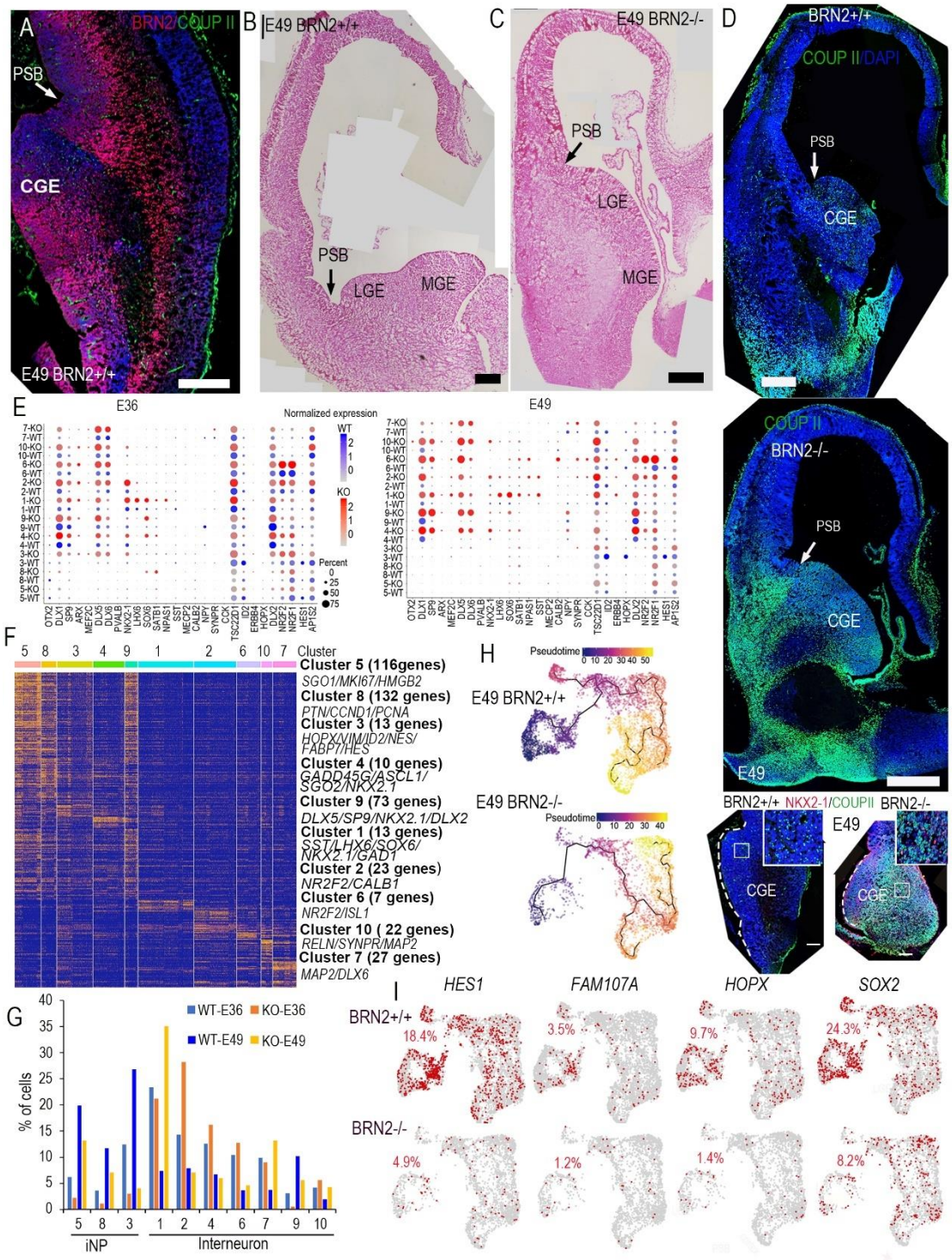

Fig. S6. *BRN2* deletion results in abnormal development of interneurons in the ganglionic eminences (GEs). (**A**) Expressions of BRN2 and COUP II (NR2F2) in the E49 fetal telencephalon, showing that BRN2 is enriched in caudal GE (CGE). PSB, pallial-subpallial boundary. (**B-D**) The same region sections were used to perform comparison analysis between *BRN2*+/+ and *BRN2*-/- telencephalon. (**B, C**) HE staining of BRN2-WT

(*BRN2*+/+) and BRN2-KO (*BRN2*-/-) telencephalon, respectively. Regionalization of LGE (lateral GE) and MGE (medial GE) was difficult to distinguish in the *BRN2*-/- monkey. (**D**) Expression of COUP II and NKX2.1 in the *BRN2*+/+ and *BRN2*-/- telencephalon. *BRN2*-mutation markedly upregulated COUPII and NKX2.1 expression in the *BRN2*-/- monkey CGE. (**E**) Dot plots of some known markers in 10 major clusters from *BRN2*+/+ and *BRN2*-/- telencephalon single cells. The left panel showed single cells of embryonic day 36 (E36) telencephalon. The right panel showed single cells of E49 telencephalon. (**F**) Differentially expressed genes specific for each cluster (also see Table S4). Representative genes were shown on the right panel. (**G**) Comparisons of cell proportions of 10 clusters between *BRN2*+/+ and *BRN2*-/- samples at different developmental stages. (**H**) UMAP visualization of cell trajectories of the *BRN2*+/+ and *BRN2*-/- samples, colored by inferred pseudo time. (**I**) The expression profiles of markers (*HES1*, *FAM107A*, *HOPX* and *SOX2*) along with the trajectories of *BRN2*+/+ and *BRN2*-/- cells in (**H**). Numbers in red indicate the ratios of positive cells (normalized expression value > 1) versus the total cell numbers. All images of immunofluorescence were from coronal sections of telencephalon. Scale bars: 500 μm. Blue: DAPI, nuclear staining.

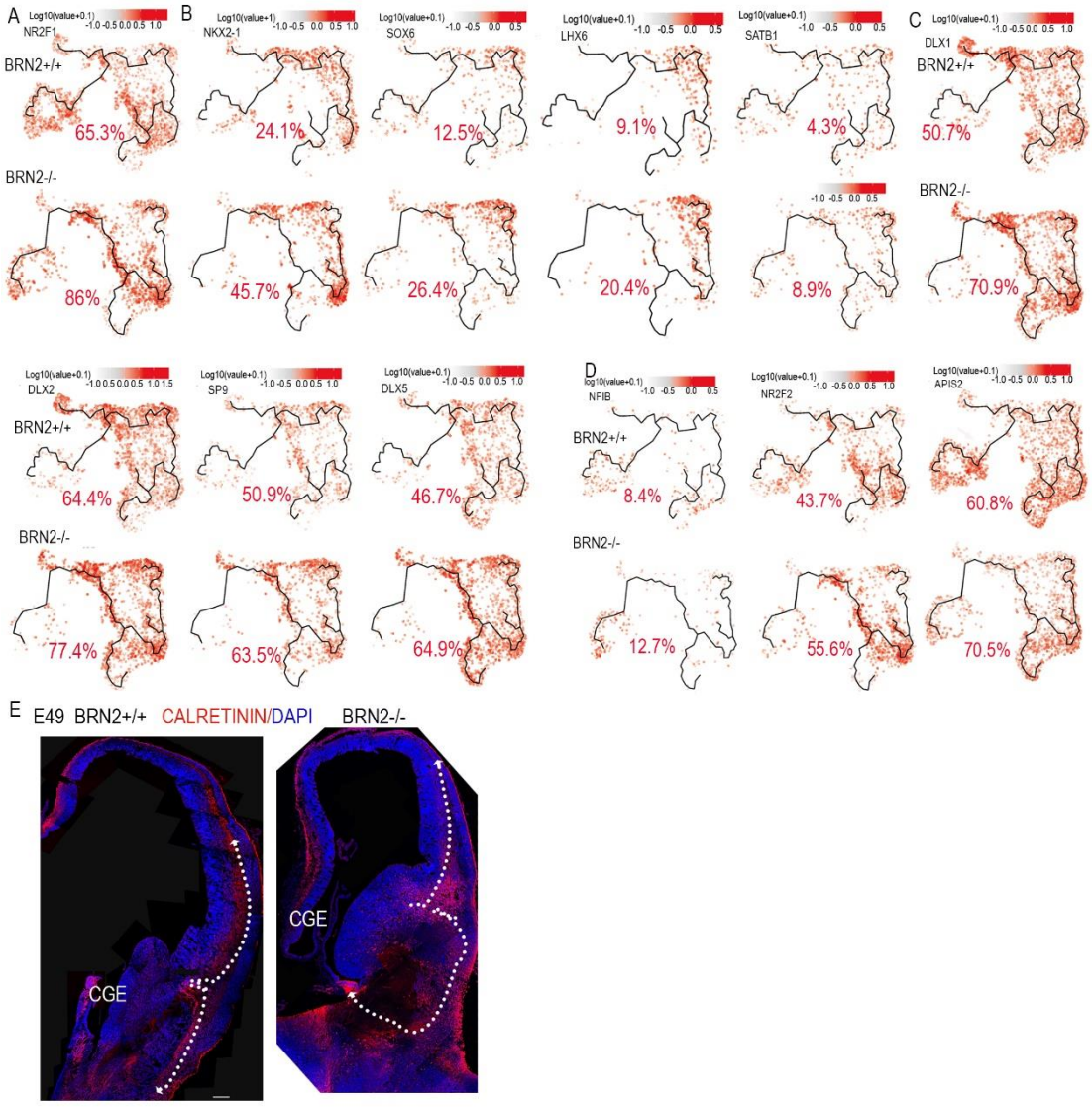

Fig. S7. *BRN2* loss promotes interneuron differentiation. (**A**) Expression of *NR2F1* as an MGE marker in the WT (*BRN2*+/+) and *BRN2*-/- (knockout) ganglionic eminence (GE) cells. (**B**) Expressions of *NKX2-1*, *SOX6*, *LHX6* and *SATB1* in the *BRN2*+/+ and *BRN2*-/- GE cells, showing that these genes were dramatically upregulated in *BRN2*-/- cells. (**C**) Expressions of *DLX1*, *DLX2*, *SP9* and *DLX5* in the *BRN2*+/+ and *BRN2*-/- GE cells, showing that these genes exhibited dramatic upregulations in *BRN2*-/- cells. (**D**) Expressions of *NR2F2*, *NFIB* and *APIS2* as CGE markers in the *BRN2*+/+ and *BRN2*-/- GE cells, showing that these genes were dramatically activated in *BRN2*-/- cells. (**E**) Differentiation and migration of calretinin (CR) interneurons in the *BRN2*+/+ and *BRN2*-/- GEs, respectively. The white dotted line arrowheads indicate the orientations of CR interneuron migration. The same region sections

were used to perform comparison analysis between *BRN2*+/+ and *BRN2*-/- telencephalon. Numbers in red indicate the ratios of positive cells (normalized expression value > 1) versus the total cell numbers. PSB, pallial-subpallial boundary; VZ, ventricular zone; LGE, lateral GE; MGE, medial GE; CGE, caudal GE. Scale bars: 500 μm. Blue: DAPI, nuclear staining.

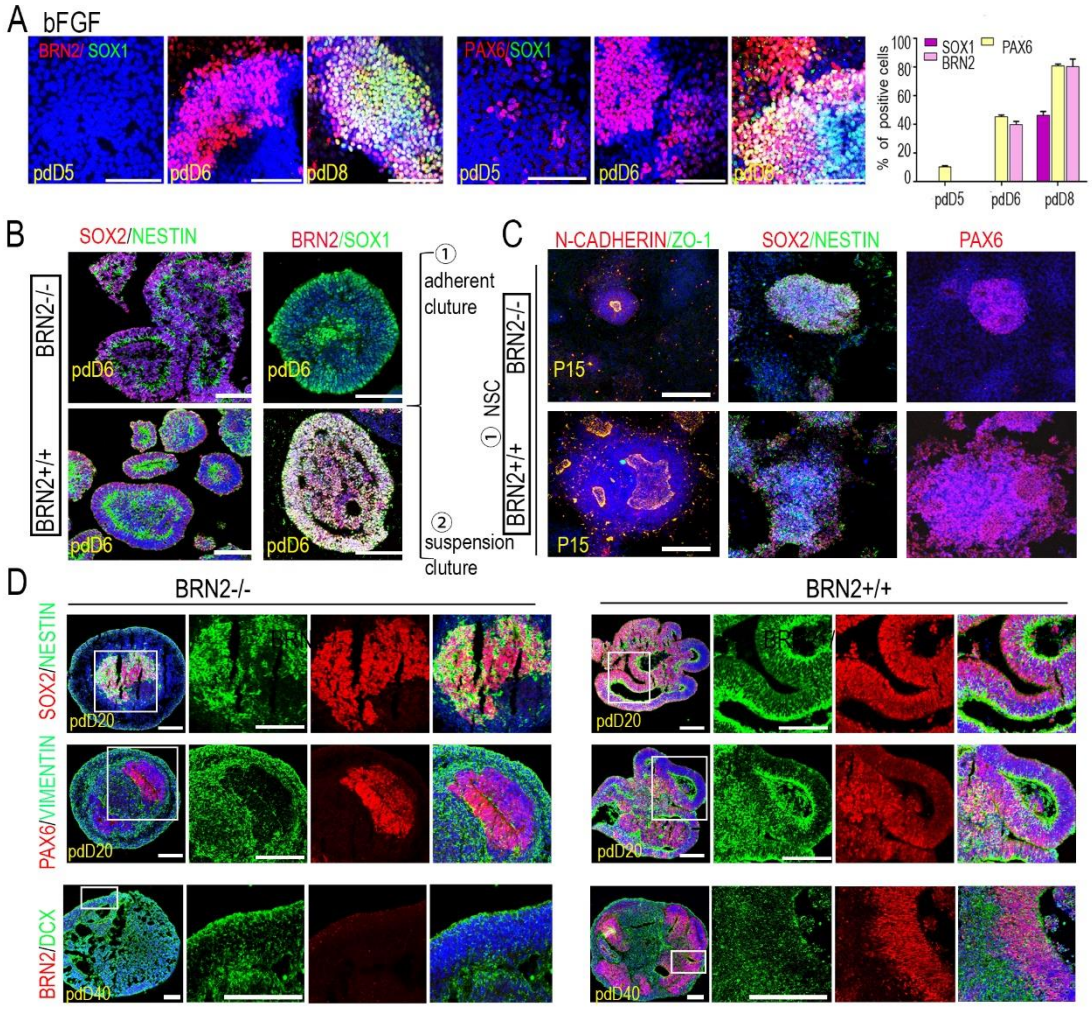

Fig. S8. *BRN2* deletion disrupts the development of human ESC-derived cortical organoids, related to Figure 5. (**A**) Dynamic expressions of PAX6, SOX1 and BRN2 during the course of human ESC differentiation into neuroectoderm in the bFGF condition. The right panel showed quantification of BRN2, SOX1 and PAX6 positive cells during the course of neural differentiation from human ESCs in the bFGF condition. Data were presented as mean ± SEM (n=3). (**B**) Immunostainings of the neuro-bodies at pdD6 with SOX2, NESTIN, SOX1 and BRN2. No obvious difference of SOX2, NESTIN and SOX1 expression was observed in the differentiated neuro-bodies from *BRN2*-/- and *BRN2*+/+ ESCs, implying that BRN2 deletion did not affect the generation of neuroepithelium cells. The neuro-bodies were subsequently conducted adherent culture (**C**) and suspension culture (**D**), respectively. (**C**) For adherent culture, neuro-bodies were digested into single cells for extensive expansion. Cells at passage 15 were immunostained with N-CADHERIN, ZO-1, SOX2, NESTIN and PAX6.

Most of *BRN2*-/- cells lost the neural progenitor identity whereas *BRN2*+/+ cells still maintained the neuroepithelium identity. (**D**) For suspension culture, the neuro-bodies were continuously cultured for 14 or 34 days to generate cortical organoids. The corticalex organoids were immunostained with SOX2, NESTIN, PAX6, VIMENTIN, BRN2 and DCX between *BRN2*-/- and *BRN2*+/+ ESCs at pdD20 and pdD40. Immounstaing data showed that BRN2 loss disrupts the development of human ESC-derived cortex organoids by losing the neuroepithelium identity and promoting the neuron precious differentiation. Scale bars: 100μm. Blue: DAPI, nuclear staining.

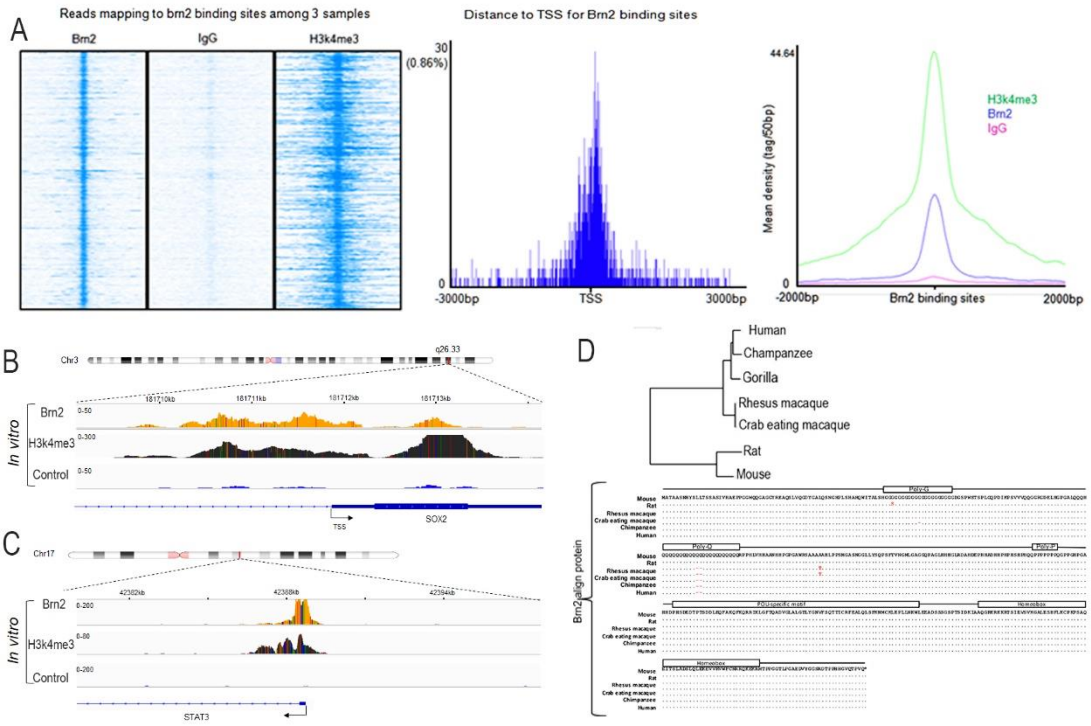

Fig. S9. The Chip-Seq data of BRN2 in human cortical cells and NESCs, related to Fig 6. (A) Representative data for CUT&Tag chromatin profiling of BRN2, IgG and H3K4me3 inhuman ESC-derived NESC. **(B)** Gene plots showing BRN2, H3K4me3, and IgG (the control) density at the *SOX2* promoter in human ESC-derived NESCs. **(C)** Gene plots showing BRN2, H3K4me3, and IgG (the control) density at the *STAT3* promoter in human ESC-derived NESCs. **(D)** The phylogenetic tree and sequence alignment of *BRN2* across different species indicate that *BRN2* is evolutionarily conserved.

Supplemental Tables

Table S1. The off-target information of *BRN2*-/- fetal monkeys, Relative to Fig. 2

(S1-1) and (S1-2) show the potential off-target sites list of sgRNA-A and sgRNA-C obtained from http://www.rgenome.net/cas-offinder/ at the condition that mismatch number equal to or less than 3 and DNA/RNA bulge Size equal to or less than 2. (S1-3) and (S1-4) show the selected 20 potential off-target sites for testing; (S1-5) PCR primers information and sequencing results of the 20 off--target sites listed in (S1-3) and (S1-4).

Table S2. Information of single-cell RNA-seq used in this study, relative to supplemental Fig. 4.

(S2-1) Differentially expressed genes of 22 clusters in E29 samples (Relative to supplemental Fig. 4B)

(S2-2) Cell proportions and identities of 22 clusters in E29 samples (Relative to supplemental Fig. 4C)

(S2-3) Differentially expressed genes of 24 clusters in integrated data from *BRN2*+/+ and *BRN2*-/- telencephalons across three stages (Relative to supplemental Fig. 4D)

(S2-4) Cell proportions and identities of 24 clusters in integrated data from *BRN2*+/+ *and BRN2*-/- telencephalons across three stages (Relative to supplemental Fig. 4D)

Table S3. Differentially expressed genes of cortical cells, relative to Figure 3.

(S3-1) Differentially expressed genes were used to identify 13 clusters of RGs and excitatory neurons (Relative to Fig. 3E)

(S3-2) Cell proportions and identities of 13 clusters (Relative to Fig. 3H)

(S3-3) Specifically expressed genes used in the heatmap of 13 clusters in supplemental Fig. 5E

(S3-4) The upregulated and downregulated genes in *BRN2*-/- cortical cells, compared to *BRN2*+/+ cortical cells at E29 (Relative to Fig. 3J)

(S3-5) The upregulated and downregulated genes in *BRN2*-/- cortical cells, compared to *BRN2*+/+cortical cells at E36. (Relative to Fig. 3J)

(S3-6) The upregulated and downregulated genes in *BRN2*-/- cortical cells, compared to *BRN2*+/+ cortical cells at E49 (Relative to Fig. 3J)

(S3-7) The upregulated and downregulated transcription factors in BRN2-/- cells, compared to *BRN2*+/+ cells at different stages (Relative to Fig. 3J)

(S3-8) Gene Ontology terms of upregulated and downregulated genes in BRN2-/- cells, compared to BRN2+/+ cells at E29, E36 and E49 (Relative to Fig. 3J)

(S3-9) KEGG pathways of upregulated and downregulated genes in BRN2-/- cells, compared to BRN2+/+ cells at E29, E36 and E49 (Relative to Fig. 3J)

Table S4. Differentially expressed genes in *BRN2*-/- interneurons, compared to *BRN2*+/+ interneurons, relative to Figure 4 and S6.

(S4-1) Differentially expressed genes were used to identify 10 clusters of interneuron progenitors (iNPs) and interneurons (Relative to Fig. 4)

(S4-2) Specifically expressed genes used in the heatmap of 10 clusters (Relative to supplemental Fig. 6G)

(S4-3) Cell proportions of 10 clusters in iNPs and interneurons (Relative to supplemental Fig. 6H)

(S4-4) Comparison of the upregulated and downregulated genes in *BRN2*-/- and *BRN2*+/+ iNPs and interneurons at E36 and E49 (Relative to Fig. 4E)

(S5-5) The upregulated and downregulated transcription factors in *BRN2*-/- iNPs and interneurons, compared to *BRN2*+/+ iNPs and interneurons at different stages (Relative to Fig. 4E)

(S4-6) Gene Ontology terms of upregulated and downregulated genes in *BRN2*-/- iNPs and interneurons at E36 and E49 (Relative to Fig. 4E)

(S4-7) KEGG pathways of upregulated and downregulated genes in *BRN2*-/- iNPs and interneurons at E36 and E49 at E36 and E49 (Relative to Fig. 4E)

Table S5. ChIP-Seq bound regions called for BRN2 and H3K4ME3 in NESCs, related to Fig. 6C.